Neurobiology of Disease 171 (2022) 105748

Contents lists available at ScienceDirect

Neurobiology of Disease

journal homepage: www.elsevier.com/locate/ynbdi

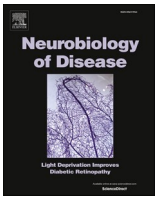

Association between lower body temperature and increased tau pathology in cognitively normal older adults

Esther M. Blessing [a,*], Ankit Parekh [b], Rebecca A. Betensky [c], James Babb [d], Natalie Saba [a], Ludovic Debure [d], Andrew W. Varga [b], Indu Ayappa [b], David M. Rapoport [b], Tracy A. Butler [e], Mony J. de Leon [e], Thomas Wisniewski [d], Brian J. Lopresti [f], Ricardo S. Osorio [a,d]

[a] Department of Psychiatry, NYU Grossman School of Medicine, New York, NY 10016, United States of America
[b] Mount Sinai Integrative Sleep Center, Division of Pulmonary, Critical Care, and Sleep Medicine, Icahn School of Medicine at Mount Sinai, One Gustave L. Levy Place, New York, NY 10029, United States of America
[c] Department of NYU School of Global Public Health, New York, NY 10016, United States of America
[d] Alzheimer's Disease Research Center, Department of Neurology, NYU Grossman School of Medicine, New York, NY 10016, United States of America
[e] Department of Neurology, Weill Cornell Medicine, New York, NY 10065, United States of America
[f] Department of Radiology, University of Pittsburgh, Pittsburgh, PA 15213, United States of America

ARTICLE INFO

Keywords:
Tau
Phosphorylation
Body temperature
Aging
Alzheimer's disease
Neurofibrillary tangle
[^{18}F]MK-6240

ABSTRACT

Background: Preclinical studies suggest body temperature (Tb) and consequently brain temperature has the potential to bidirectionally interact with tau pathology in Alzheimer's Disease (AD). Tau phosphorylation is substantially increased by a small (<1 °C) decrease in temperature within the human physiological range, and thermoregulatory nuclei are affected by tau pathology early in the AD continuum. In this study we evaluated whether Tb (as a proxy for brain temperature) is cross-sectionally associated with clinically utilized markers of tau pathology in cognitively normal older adults.

Methods: Tb was continuously measured with ingestible telemetry sensors for 48 h. This period included two nights of nocturnal polysomnography to delineate whether Tb during waking vs sleep is differentially associated with tau pathology. Tau phosphorylation was assessed with plasma and cerebrospinal fluid (CSF) tau phosphorylated at threonine 181 (P-tau), sampled the day following Tb measurement. In addition, neurofibrillary tangle (NFT) burden in early Braak stage regions was imaged with PET-MR using the [18F]MK-6240 radiotracer on average one month later.

Results: Lower Tb was associated with increased NFT burden, as well as increased plasma and CSF P-tau levels ($p < 0.05$). NFT burden was associated with lower Tb during waking ($p < 0.05$) but not during sleep intervals. Plasma and CSF P-tau levels were highly correlated with each other ($p < 0.05$), and both variables were correlated with tau tangle radiotracer uptake ($p < 0.05$).

Conclusions: These results, the first available for human, suggest that lower Tb in older adults may be associated with increased tau pathology. Our findings add to the substantial preclinical literature associating lower body and brain temperature with tau hyperphosphorylation. Clinical trial number: NCT03053908.

Abbreviations: AD, Alzheimer's Disease; AHI, Apnea-Hypopnea Index; BMI, Body mass index; CDR, Clinical Dementia Rating; CSF, Cerebrospinal fluid; DRAGO, Data with Random Gaps and Outliers; ESS, Epworth Sleepiness Scale; LP, Lumbar puncture; MCI, Mild cognitive impairment; MMSE, Mini-Mental State Examination; MR, Magnetic resonance; NFT, Neurofibrillary tangle; NPSG, Nocturnal polysomnography; OSA, Obstructive sleep apnea; PET, Positron emission tomography; P-tau, Tau phosphorylated at threonine 181; Tb, Body temperature; TimeSubThr, Percent of time body temperature is under threshold; SUVR, Standardized uptake volume ratio.

* Corresponding author.
E-mail addresses: esther.blessing@nyulangone.org (E.M. Blessing), ankit.parekh@mssm.edu (A. Parekh), rebecca.betensky@nyu.edu (R.A. Betensky), james.babb@nyulangone.org (J. Babb), natalie.saba@nyulangone.org (N. Saba), ludovic.debure@nyulangone.org (L. Debure), andrew.varga@mssm.edu (A.W. Varga), indu.ayappa@mssm.edu (I. Ayappa), david.rapoport@mssm.edu (D.M. Rapoport), tab2006@med.cornell.edu (T.A. Butler), mdl4001@med.cornell.edu (M.J. de Leon), Thomas.Wisniewski@nyulangone.org (T. Wisniewski), brianl@pitt.edu (B.J. Lopresti), Ricardo.Osorio@nyulangone.org (R.S. Osorio).

https://doi.org/10.1016/j.nbd.2022.105748
Received 4 January 2022; Received in revised form 25 April 2022; Accepted 5 May 2022
Available online 10 May 2022

1. Background

Neurofibrillary tangles (NFTs), comprised of hyperphosphorylated aggregated tau protein, are the pathological hallmark of neurodegenerative tauopathies including Alzheimer's Disease (AD) (Grundke-Iqbal et al., 1986; Scheltens et al., 2021). The presence of NFTs, as evidenced by in vivo tau PET imaging, predicts both grey matter volume loss and clinical progression in AD, suggesting NFTs or their soluble tau oligomer precursors promote neurodegeneration (Ossenkoppele et al., 2016; Pascoal et al., 2017; Clark et al., 2021; Ossenkoppele et al., 2021). Tau is a natively soluble protein that binds to microtubules to stabilize the cytoskeleton and facilitate intracellular trafficking (Guo et al., 2017; Dixit et al., 2008; Vershinin et al., 2007), and may also regulate synaptic plasticity (Kimura et al., 2014; Biundo et al., 2018). Tau's function is modulated by alternative RNA splicing, and by post-translational enzymatic modifications including phosphorylation at over 40 serine and threonine phosphorylation sites (Gong et al., 2005; Gotz et al., 2019). Tau hyperphosphorylation is likely to be pathological, given it is observed in soluble precursors of NFTs, and also promotes tau's detachment from microtubules and subsequent aggregation (Gong and Iqbal, 2008; Lindwall and Cole, 1984; Augustinack et al., 2002; Wegmann et al., 2021). Mechanisms driving tau hyperphosphorylation are not well understood. Increasing age (Braak and Braak, 1997), apolipoprotein E (*APOE* genotypes) (Clark et al., 2021), amyloid beta deposition (van der Kant et al., 2020; Janelidze et al., 2020), and cerebrovascular disease (Laing et al., 2020) have been implicated at the patient level, and imbalances in the activity of tau kinases (Shukla et al., 2012) and phosphatases (Sontag and Sontag, 2014), at the molecular level.

Temperature, a function of the average speed at which molecules undergo Brownian motion, potently influences tau phosphorylation. Laboratory animal and in vitro experiments over the last 20 years show that a small (< 1 °C) decrease in temperature within the human physiological range substantially increases neuronal tau phosphorylation at sites that are hyperphosphorylated in AD patients (Planel et al., 2004; Planel et al., 2007; Gratuze et al., 2017; Tournissac et al., 2017; Hitrec et al., 2021; Luppi et al., 2019). In vivo, tau phosphorylation is increased by body temperature (Tb) and consequent brain temperature decreases accompanying hibernation (Arendt et al., 1995; Stieler et al., 2011), sleep (Guisle et al., 2020), and hypoglycemia (Planel et al., 2004). These effects are prevented by maintaining Tb with heating. Regarding mechanism, decreasing Tb inhibits the activity of the major tau phosphatase (PP2A) more so than tau kinase activity, resulting in a net phosphorylation increase (Planel et al., 2004; Planel et al., 2001). Importantly, decreasing temperature by <1 °C robustly increases phosphorylation at AD relevant sites on human neuronal tau in vitro (Guisle et al., 2020; Bretteville et al., 2012), suggesting that lower human Tb and brain temperature could increase tau phosphorylation and potentially, tau pathology.

Whether lower Tb is associated with tau pathology in human has not yet been reported. In wild-type laboratory animals, tau phosphorylation associated with hypothermia is usually reversible upon return to euthermia (Luppi et al., 2019; Arendt et al., 1995). However, this reversibility may be impaired in the setting of persistent hypothermia, e.g. that associated with aging (Weitzman et al., 1982; Kenney and Munce, 2003; Blatteis, 2012; Gomolin et al., 2005), or by molecular alterations associated with age or AD, as previously suggested (Tournissac et al., 2017; Stieler et al., 2011; Arendt et al., 2015) and demonstrated in a mouse model of tauopathy (Planel et al., 2009). Therefore, lower Tb or disturbed Tb circadian rhythm may be a mechanism whereby age and age-related conditions increase the risk of AD. Further, mitigating thermoregulatory impairment in older adults with targeted Tb interventions could prevent NFT formation (Tournissac et al., 2019). Finally, relevant to understanding disease progression, a bidirectional relationship may exist between thermoregulatory dysfunction and AD pathology (Tournissac et al., 2017; Vandal et al., 2016). Body temperature alterations have been reported in late-stage AD (Mishima et al., 1997; Harper et al., 2005; Prinz et al., 1984; Volicer et al., 2012; Harper et al., 2008; Satlin et al., 1995; Touitou et al., 1986; Okawa et al., 1991; Harper et al., 2004), but so far there are no reports of temperature in preclinical or early AD.

Here, in cognitively normal older adults, we tested whether lower Tb is associated with increased aggregated (tau radiotracer uptake) and soluble (plasma and CSF) tau pathology. Neurofibrillary tangle burden in Braak I–III stage brain regions was visualized with PET-MR imaging using the tau radiotracer [^{18}F]MK-6240 (MK6240) (Pascoal et al., 2020; Betthauser et al., 2020; Yap et al., 2021), which has sub-nanomolar affinity for hyperphosphorylated tau in paired helical filament formation (Hostetler et al., 2016; Pascoal et al., 2018). Soluble markers of tau burden and tau phosphorylation included cerebrospinal fluid (CSF) and plasma tau phosphorylated at threonine 181 (P-tau). Like CSF P-tau, plasma P-tau is elevated prior to tau PET positivity and predicts future neurodegeneration and dementia onset (Janelidze et al., 2020; Karikari et al., 2020). Tb was continuously measured with ingestible telemetry (Huang et al., 2021; Travers et al., 2016; Monnard et al., 2017) for up to 48 h. Given reports of sleep-wake variation in tau phosphorylation in wild-type mice (Guisle et al., 2020), sleep-wake state was assessed with nocturnal polysomnography (NPSG) on both nights of this 48 h period to delineate whether tau pathology was differentially associated with Tb measured during sleep vs waking intervals.

2. Materials & methods

2.1. Participants and screening procedures

Subjects were recruited from the NYU Cohort, comprised of community dwelling cognitively normal volunteers derived from NIH/National Institute on Aging and Alzheimer's Association supported studies. Data were collected from an ongoing cross-sectional observational study (R21AG055002) designed to assess the association between sleep parameters and tau pathology in cognitively normal older adults. All participants underwent medical, psychiatric, neurological and neuropsychological assessments; genetic testing for *APOEε4* status, and assessment for daytime somnolence with the Epworth Sleepiness Scale (ESS) (Johns, 1991).

Medical screening included medical history, examination and routine blood tests, electrocardiogram, height and weight, and MRI. Exclusion criteria included a history of brain tumor; MRI evidence of brain damage or other serious neurological disorder; significant history of alcoholism or drug abuse or current alcoholism or drug abuse; a history of major psychiatric illness; Geriatric Depression Scale (short form) >5; obesity (Body mass index >30); insulin dependent diabetes; family history of early onset dementia; evidence of clinically relevant cardiac, pulmonary, endocrine or hematological conditions including thyroid disorders; irregular sleep-wake rhythms (based on 7 day home actigraphy recordings prior to lab visits) or significant obstructive sleep apnea (AHI4% $\geq$ 15); and medications known to affect thermoregulation or sleep.

Cognitive screening included the Mini—Mental Status Examination, Clinical Dementia Rating scale and other elements of the National Alzheimer's Coordinating Center (NACC) Uniform Data Set Neuropsychological Test Battery. The diagnosis of cognitively normal was made by an experienced clinician according to standard criteria, and based on the diagnostic interview with the participant and his/her study partner, together with review of all available information including cognitive test scores and neuroimaging.

2.2. Integrated body temperature and sleep-wake state measurement

Core body (gastrointestinal tract) temperature was measured with CorTemp ingestible pill-shaped telemetric sensors (CorTemp H.Q., Palmetto, FL) monitored by a wearable data recorder. Body temperature was continuously measured for up to 48 h, sampling every 10 s with an

accuracy of ± 0.2 °C. This 48 h period (the 'Total' Tb interval) included two nights of NPSG in the sleep lab (the 'Sleep' interval) and the two subsequent days (the 'Waking' interval), see Fig. 1. During the Waking interval, participants chose their location and behaved, i.e., ate, exercised and showered according to their usual schedule. Participants were asked to wear the Tb monitor, avoid naps, stay out of range of electronic devices, and complete a temperature log of events that might affect Tb recording. See Supplementary File 1 for further details.

2.3. Body temperature data processing and features

Data were excluded by a researcher blind to tau data from participants with less than 24 h of recording, or within 1 h of the participant changing over sensors or the receiver being out of range. Data were then processed with '**DRAGO**' (nonlinear smoothing of **D**ata with **RA**ndom **G**aps and **O**utliers), developed by co-author Dr. Ankit Parekh for identifying outliers and gaps caused by signal interference and loss (Parekh, 2021). DRAGO processed data were edited by a blind rater to correct obvious errors in fit where present. Circadian parameters were calculated to establish whether DRAGO processed data yielded plausible circadian parameters, see Supplementary File 1 for further details of this analysis and DRAGO.

Six features were calculated from DRAGO processed Tb data: 1–3) Mean Tb for Total, Sleep, and Waking intervals, and 4–6) The proportion (%) of temperature data points below a specified temperature threshold (37 °C) for each of these intervals, termed time of subthreshold temperature, or TimeSubThr. We chose a threshold of 37 °C given temperatures below this value were shown to cause hyperphosphorylation in rodent and human tau assays (Planel et al., 2004; Planel et al., 2008). The final threshold used for data analyses was that both closest to 37.0 °C and to the mean Tb for that interval in the final sample. This threshold was 37.0 °C for the Total interval, 36.8 °C for the Sleep interval, and 37.1 °C for the Waking interval. To ensure against spurious findings, neighboring thresholds +/− 0.1 °C (and closest to 37.0 °C) were tested, with the idea that a 0.1 °C difference is below the accuracy of Tb measurement (0.2 °C), so should not substantially affect correlations. Results for a given Tb–tau pathology correlation were considered significant if at least one other neighboring threshold was significant at $p < 0.05$.

2.4. Tau tangle PET-MR imaging

PET-MR scans occurred within 29 ± 18 days of Tb measurement. See Supplementary File 2 for further details of PET-MR image processing. Briefly, standard uptake value ratio (SUVR) values from images acquired during the 90–110 min post-injection interval were computed for all FreeSurfer regions, normalizing to cerebellar grey matter. MR-based partial volume correction (PVC) was performed using Rousset's geometric matrix transfer method (Rousset et al., 1998). Data were analyzed from composite regions corresponding to Braak pathological stages I–III, their constituent right and left hemisphere brain subregions (Braak I: entorhinal cortex; Braak II: hippocampus; Braak III: parahippocampal gyrus, amygdala, fusiform gyrus, lingual gyrus), and control brain regions not expected to contain NFTs including the pericalcarine cortex, corpus callosum, and caudate nucleus. Partial volume corrected data were used for the main analysis given the higher signal to noise ratio; results from uncorrected data are also presented. Data from left hemisphere brain regions are presented in the main manuscript, and from right hemisphere regions, in supplementary materials.

2.5. Plasma and CSF P-tau assays

Fluoroscopically-guided lumbar punctures followed by venous blood samples were performed in the morning to early afternoon the day following Tb assessment using previously described procedures (Spiegel et al., 2016; Vanderstichele et al., 2012). This time of sampling was chosen to follow the ADNI guidelines recommending morning sampling (Hansson et al., 2018), which is also the consensus for clinical practice and the literature (Vanderstichele et al., 2012). Concentrations of CSF and plasma tau phosphorylated at threonine 181 (P-tau) were measured using Simoa HD-X instruments (Quanterix, Billerica, MA, USA) at the NYU Alzheimer's Disease Center Biomarker Core according to the manufacturer's instructions. See Supplementary File 2 for further details.

2.6. Statistical analyses

Data analyses were performed using Matlab version R2020b (Mathworks, Inc., Natick, MA). Data were examined for outlier status (values less than the first quartile minus 1.5 x the interquartile range, or values greater than the third quartile plus 1.5 x the interquartile range) and tested for deviation from a normal distribution using the Shapiro-Wilk test. Roughly half of the variables examined either had outliers or non-normal distributions, thus non-parametric (Spearman rank) correlations (robust against outliers) were used for all correlations. Correlations driven by a single outlier value were rejected if results were not significant with this value deleted. Correlations involving Total Tb data were corrected via partial correlation by the ratio of time spent asleep vs awake, given participants who spent more time asleep had lower Total mean Tb ($r = -0.53$, $p < 0.05$) and higher Total TimeSubThr ($r = 0.62$, $p < 0.05$). To account for potential confounds, which included *APOε4* carrier status, BMI, age, sex, ethnicity, education, ESS, and AHI3a (sleep apnea), these variables were first correlated with the dependent and independent variable in all correlations. Resulting correlations were weak–moderate ($r < 0.45$) and non-significant ($p > 0.1$), meaning that no partial correlations were required; however, we note that when

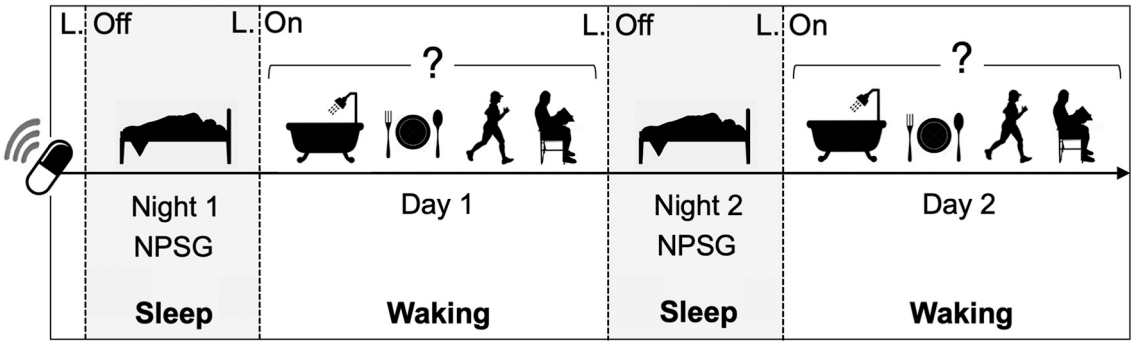

Fig. 1. | Protocol for integrated measurement of body temperature and sleep. Time of body temperature sensor (pill) ingestion and recording indicated by line continuing from pill. Nocturnal polysomnography (NPSG) on Nights 1 and 2. Sleep interval (grey) included time between lights off (L. Off) and lights on (L. On), occurring in the sleep lab during NPSG. The Waking interval (white) included time on Days 1 and 2 between lights On and lights Off. During this time, subjects were free to return home and behave according to their normal schedule, indicated by activities bracketed under '?'.

Tb–tau pathology correlations were corrected for these potential confounds, correlations were not diminished in magnitude or significance.

3. Results

3.1. Participant characteristics

The final participants (all those who completed PET-MR imaging) were $n = 21$ community dwelling cognitively normal volunteers (81% female) of mean age 65.4 ± 5.2 years, with 38% *APOε4* carriers, mean BMI = 25.4 ± 3.5, minimal daytime sleepiness and normal thyroid function at the time of screening, see Table 1 for participant characteristics. Several participants had mild or moderate sleep apnea (median AHI3a 6.43). All participants except for one had a Clinical Dementia Rating (CDR) score of 0; the mean Mini-Mental State Examination (MMSE) was 29.04 ± 1.4. One participant with CDR of 0.5 had a MMSE of 26. The amyloid beta status of participants, i.e., whether they exceeded preclinical AD thresholds for CSF or PET amyloid beta load, was unknown.

3.2. Relationship between tau PET, plasma P-tau and CSF P-tau markers

MK6240 PET-MR images were collected in 21 participants, plasma P-tau levels in 19, and CSF P-tau levels in 20 participants, see Table 2 and Fig. 2. Three of 19 subjects were positive according to CSF P-tau cut-offs for 'T' status in preclinical AD (60 pg / mL) (Hansson et al., 2006). Fig. 2 shows fused PET and MR images for example T+ and T- subjects. Artifactual meningeal uptake was present in participants both with and without MK6240 parenchymal uptake, as previously reported (Gogola et al., 2021). Neither Braak composite region MK6240 PET SUVR values, nor CSF, nor plasma P-tau levels were associated with age in the current sample ($r < 0.30$, $p > 0.05$ for all comparisons). There were strong associations ($r = 0.45$–0.8, $p < 0.05$) between soluble P-tau measures, and between soluble measures and MK6240 SUVR uptake in most Braak I-III composite regions and constituent subregions (Fig. 2, Table S1 in Supplementary File 3).

Table 1
Participant characteristics.

	n = 21
Age	65.4 ± 5.2
Female	17 (81%)
BMI	24.05 ± 4.1
Education	17.3 ± 1.8
CDR	0.02 ± 0.1
GDS	1.8 ± 0.5
MMSE	29.04 ± 1.4
ApoE4+	8 (38%)
Sleep	
AHI3a	8.14 ± 7.1
ESS	4.4 ± 3.2
Comorbidities	
Hypertension	*3 (14%)*
Cardiovascular Disease	1 (5%)
Diabetes	1 (5%)
Thyroid Disorders	4 (19%)
Race	
White	19 (90%)
Black	2 (10%)
Medications	
Antidepressants	7 (33%)
Statins	7 (33%)
Antidiabetic	1 (5%)
Antihypertensive	3 (14%)
Thyroid	4 (19%)

Table 1 | Results reported as mean ± SD or n (%). Abbreviations: BMI, body mass index, CDR, Clinical Dementia Rating, MMSE, Mini Mental State Examination, ESS, Epworth Sleepiness Scale, AHI3a, Apnea Hypopnea Index with 3% Desaturation, GDS, global dementia scale.

3.3. Reliability of telemetric Tb assessment including DRAGO data processing

Acceptable Tb data were collected for 15/21 participants, all with at least 33 h data acquired (mean 46.27 ± 15.6 h). Of the remaining six, two had Tb data <24 h, two did not return the receiver, and in two, highly irregular Tb traces indicated receiver malfunction. Fig. 3 shows raw and DRAGO processed Tb data for one participant. DRAGO accurately filled data gaps and excluded outlier values in almost all (14/15) participants. Manual editing was required for one participant. Both direct and cosine analyses of DRAGO outputs yielded circadian parameters consistent with previous studies of circadian rectal Tb (Touitou et al., 1986; Weinert, 2010; Kelly, 2006). (Table S2, Supplementary File 3). Amplitude calculated from DRAGO outputs was ~1.5 x greater than that derived from cosine analysis, as in previous studies (Refinetti et al., 2007).

Total Mean Tb (mean 37.03 ± 0.17 °C) agreed with previous studies of rectal Tb (Touitou et al., 1986; Kelly, 2006; Sund-Levander et al., 2002). Waking Mean Tb (37.31 ± 0.17 °C) was higher than Total Mean Tb, whereas Sleep Mean Tb was lower (36.64 ± 0.15 °C), $p < 0.05$ both comparisons, see Table 2. Total TimeSubThr was on average 47.67 ± 10.5%, consistent with the average Total Mean Tb near 37 °C (and threshold of 37 °C). Waking TimeSubThr (18.2 ± 9.4%) was higher than both Total TimeSubThr and Sleep TimeSubThr (92.31 ± 10.20%) $p < 0.05$ for both comparisons. TimeSubThr was inversely related to mean Tb for all intervals ($r < 0.5$, $p < 0.01$ for all comparisons). For all intervals, Tb was not significantly and only weakly correlated with age, ESS, BMI, or the average temperature for New York City in the month of Tb measurement ($r < 0.35$, $p > 0.10$ for all comparisons), except for the correlation between ESS and mean Total Tb, which was moderate but still non-significant ($r = -0.40$, $p = 0.12$).

3.4. Association between lower Tb and greater soluble and aggregated tau pathology

Associations between Tb and tau measures were examined separately for each interval, results are shown in Figs. 4 and 5 and correlations are tabulated in Tables S3–S8, Supplementary Files 3 and 4. Greater Total TimeSubThr was strongly ($r = 0.6$–0.7) and significantly ($p < 0.05$) associated with plasma and CSF P-tau or aggregated tau, this Tb feature was strongly (r = 0.6–0.7) and significantly ($p < 0.05$) associated with SUVR uptake in the Braak II region and bilateral hippocampi, and in Braak III parahippocampal gyrus and amygdala subgregions. Total TimeSubThr was moderately ($r = 0.5$–0.59) associated with SUVR uptake in Braak I and III regions at a trend level ($p < 0.1$), and weakly ($r = 0.30$–0.45) and non-significantly ($p > 0.1$) associated with SUVR uptake in Braak III subregions lingual and fusiform gyrus. Lower Total Mean Tb was weakly ($r > -0.39$) associated with plasma and CSF P-tau at a non-significant level ($p > 0.10$), and moderately (r between −0.4 and − 0.5) associated with Braak I-III SUVR regional and subregional uptake at a trend ($p < 0.10$) or non-significant ($p > 0.10$) level. No Total Tb feature was associated with SUVR uptake in control brain regions at greater than a weak strength (all $r < 0.39$), and all associations were non-significant ($p > 0.05$). All SUVR uptake results were similar for right hemisphere equivalents and non-PVC data.

Greater Waking TimeSubThr was moderately (r = 0.5–0.6) associated with plasma P-tau at a trend level ($p < 0.10$), and moderately ($r = 0.4$–0.5) associated with CSF P-tau at a non-significant level ($p > 0.10$). For aggregated tau, this feature was strongly (r = 0.6–0.7) and significantly ($p < 0.05$) associated with SUVR uptake in Braak I and II regions and subregions and parahippocampal gyrus, moderately ($r = 0.50$) associated with SUVR uptake in the amygdala at a trend level ($p < 0.1$), and weakly ($r < 0.3$) and non-significantly ($p > 0.1$) associated with SUVR uptake in Braak III fusiform and lingual gyrus. Lower Waking

Table 2
Tau PET, plasma and CSF P-tau and body temperature group results

MR PET Tau MK-6240 Tracer Uptake (SUVR) ($n = 21$)								
Braak I–III			ERC	PHG	HPC	AMY	LNG	FUS
1.84 ± 0.81	0.79 ± 0.22	1.22 ± 0.34	1.74 ± 0.63	1.25 ± 0.35	0.77 ± 0.21	0.70 ± 0.34	1.23 ± 0.21	1.21 ± 0.41
Soluble P-tau Levels (pg / ml)			**Mean Tb (°C)(n = 15)**			**TimeSubThr (%)($n = 15$)**		
Plasma ($n = 19$)	CSF ($n = 20$)		Total	Waking	Sleep	Total	Waking	Sleep
1.72 ± 0.78	50.20 ± 60.55		37.03 ± 0.17	37.31 ± 0.17	36.64 ± 0.15	47.67 ± 10.50	18.20 ± 9.44	92.31 ± 10.20

Table 2 | Abbreviations: ERC, entorhinal cortex, PHG, parahippocampal gyrus, HPC, hippocampus, AMY, amygdala, LNG, lingual gyrus, FUS, fusiform gyrus, CSF, cerebrospinal fluid.

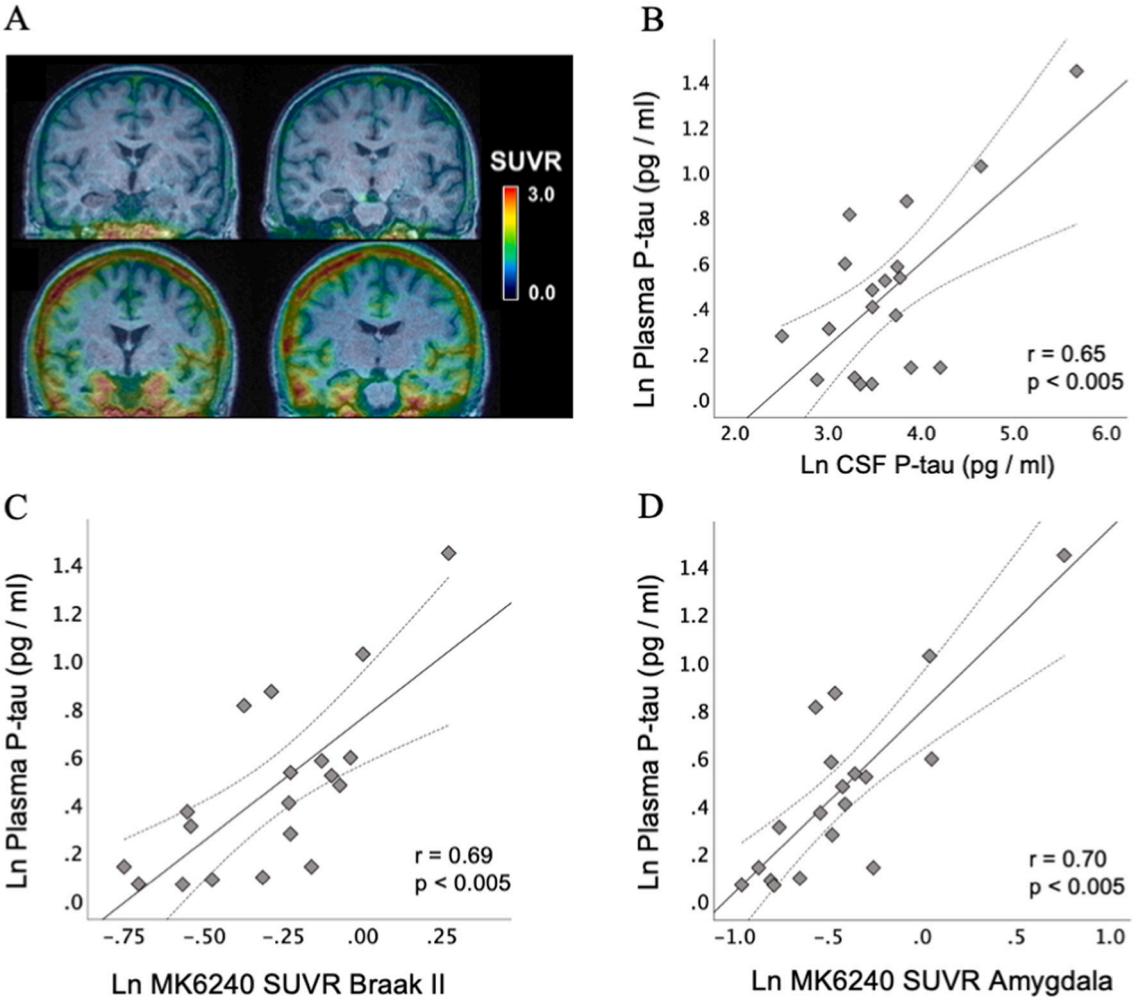

Fig. 2. Relationships between aggregated and soluble markers of tau pathology. A, Coronal [^{18}F] MK-6240 tau tangle MR-PET images from two subjects: upper, T- negative 65 yo male, lower, T+ positive 63 yo female. B-D, associations between plasma P-tau, CSF P-tau and MK6240 SUVR uptake. Solid lines show linear regression, dashed lines show mean confidence intervals. Spearman's rank correlation results at lower right of each plot.

Mean Tb was moderately ($r = -0.50$) associated with plasma P-tau at a trend level ($p < 0.1$), and moderately ($r < 0.4$) associated with CSF P-tau at non-significant level ($p > 0.1$). For aggregated tau, this feature was strongly (r between −0.6 and − 0.7) and significantly ($p < 0.05$) associated with SUVR uptake in Braak I and II regions and subregions, Braak III parahippocampal gyrus, and amygdala (r = 0.5–0.6). Waking Mean Tb was moderately ($r = -0.52$) associated with Braak III SUVR uptake at a trend level ($p < 0.1$), and weakly-moderately ($r > -0.4$) associated with SUVR uptake in the fusiform and lingual gyrus at a non-significant ($p > 0.1$) level. Similar results were obtained for right hemisphere equivalents and non-PVC data. No Waking Tb feature was associated with SUVR uptake in control brain regions at greater than a weak strength (all $r < 0.35$), and all associations were non-significant ($p > 0.05$).

For the Sleep interval, Sleep Mean Tb was only weakly ($r > -0.3$) and non-significantly ($p > 0.10$) associated with CSF and plasma P-tau and with SUVR uptake in all brain regions tested. Sleep TimeSubThr associations with all tau measures were weak-moderate (0.2–0.55) at non-

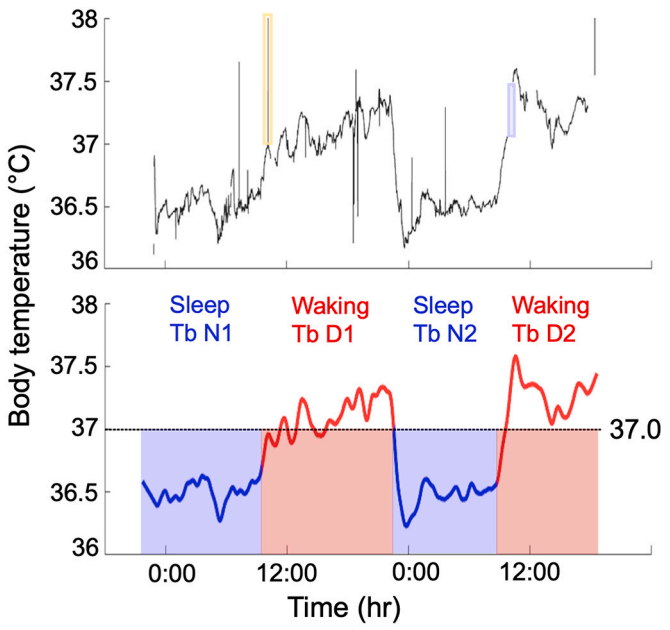

Fig. 3. | Raw and DRAGO processed body temperature data for one participant. Upper panel, raw body temperature (Tb) data, yellow shading indicates data outlier, blue shading indicates data gap. Lower panel, DRAGO processed Tb data divided into Sleep (nights 1 and 2) and Waking (days 1 and 2) intervals. Shaded areas show Tb values under indicated threshold (37 °C). Waking interval Tb metrics were Mean Tb, 37.15 °C, and time Tb under threshold (TimeSubThr), 21.44%. (For interpretation of the references to color in this figure legend, the reader is referred to the web version of this article.)

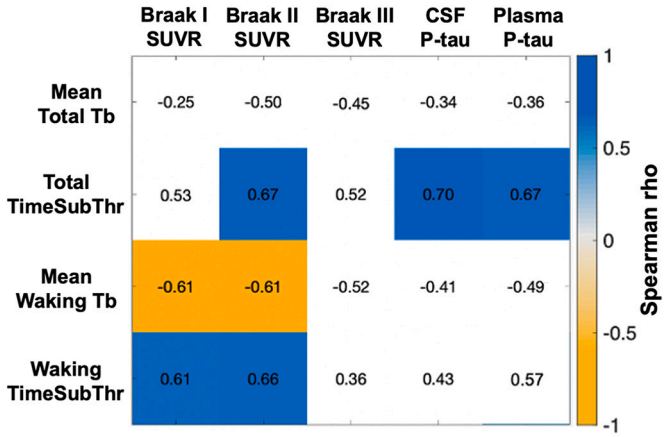

Fig. 4. | Correlation matrix of associations between body temperature, MK-6240 SUVR uptake in Braak I-III regions, CSF P-tau and plasma P-tau. Significant correlations are color coded by magnitude according to the indicated scale. Abbreviations: Tb, body temperature; SUVR, standardized uptake value ratio, TimeSubThr, body temperature under threshold. (For interpretation of the references to color in this figure legend, the reader is referred to the web version of this article.)

significant ($p > 0.1$) or trend ($p < 0.1$) levels. In summary, Tb features consistent with lower Tb were substantially, and in the majority of tests, significantly associated with increased soluble and aggregated tau pathology, with a lack of correlation in control brain regions. For the Total Tb interval, TimeSubThr was more strongly associated with both aggregated and soluble tau pathology compared to Mean Tb. For the Waking interval, both TimeSubThr and Mean Tb were strongly and significantly associated with aggregated tau pathology in most regions. By contrast, associations for the Sleep interval were relatively weak and mostly insignificant.

4. Discussion

Age-related thermoregulatory dysfunction could be an important pathophysiological pathway to Alzheimer's disease. To our knowledge, ours is the first study to relate Tb to tau pathology in humans. Lower Tb and greater tau pathology may be causally related as detailed in Fig. 6. In Arm 1 of this hypothesized bidirectional interaction, body and brain temperature directly influence the thermodynamic conditions governing tau phosphorylation and aggregation. In Arm 2, AD pathology and associated causes of thermoregulatory neuronal dysfunction cause body and brain temperature dysregulation. We discuss our results in context of both arms, following discussion of methods used to measure Tb and tau pathology.

The assays we used to measure tau pathology are state of the art biomarkers for AD diagnosis and prognosis. MK6240 (Pascoal et al., 2020; Yap et al., 2021) detects NFTs with more than twice the dynamic range of flortaucipir (Gogola et al., 2021), a widely-used FDA-approved tau radiotracer. Further, the topological pattern of MK6240 uptake more closely matches that seen in histological Braak staging, with a higher frequency of uptake in Braak I–III stages in amyloid beta negative cognitively normal and MCI older adults compared with flortacipir (Pascoal et al., 2020; Betthauser et al., 2020). While the current participant sample was limited by unknown amyloid beta status, NFT signal detection was supported by strong associations between MK6240 SUVR uptake and CSF P-tau and plasma P-tau, as previously reported for MK6240 SUVR global uptake in large samples of cognitively normal, MCI, and amyloid beta positive older adults (Karikari et al., 2020; Lee et al., 2020). Increased plasma P-tau 181 has been shown to predict detection of aggregated tau, neurodegeneration, and dementia onset with an advance of more than a decade (Janelidze et al., 2020; Barthelemy et al., 2020).

Ingestible telemetry is known to yield Tb values closely correlated with rectal and esophageal (core) Tb measures (Byrne and Lim, 2007; Gant et al., 2006; Casa et al., 2007), but has been used in few human Tb studies (Huang et al., 2021; Monnard et al., 2017), perhaps due to the need for manual removal of outliers and gap data artifacts (Monnard et al., 2017; Refinetti et al., 2007; Refinetti, 2010). Previous studies of circadian Tb variation employed oral, axillary, or skin measurement sites (unreliably related to core Tb) or rectal values (Weitzman et al., 1982; Kelly, 2006; Refinetti et al., 2007; Czeisler et al., 1980; Krauchi and Wirz-Justice, 1994; Kelly, 2007). We found that our automated telemetric Tb data processing methodology successfully dealt with these artifacts, giving a reliable measure of core Tb that closely agreed with previous studies of rectal Tb (Touitou et al., 1986; Kelly, 2006; Sund-Levander et al., 2002). We are not aware of previous studies that quantified mean Tb over the waking or sleep interval, however our values agree with point measurements during these intervals (Monnard et al., 2017). Our automated telemetric data processing method therefore advances Tb telemetry by facilitating accurate quantification of core body temperature over extended periods of time.

The goal of our study was to ascertain a sample of Tb in the context of real-life behavioral conditions typical for each participant, in order to represent preceding longer-term Tb patterns which may influence tau phosphorylation. The assumption that Tb sampled over 48 h represents longer-term Tb that is characteristic for an individual is supported by previous studies of rectal temperature (Aschoff, 1998), but requires further testing within this specific Tb measurement protocol. Toward a real-life Tb sample, we included in our data analysis Tb variations associated with the sleep-wake transition, physical activity, and other Tb-impacting behaviors usual for each participant. Our approach contrasts with studies using Tb as a marker of the endogenous circadian system, in which constant routines and data exclusion are used to minimize 'masking' effects of Tb-impacting behaviors (Krauchi and Wirz-Justice, 1994; Duffy and Dijk, 2002).

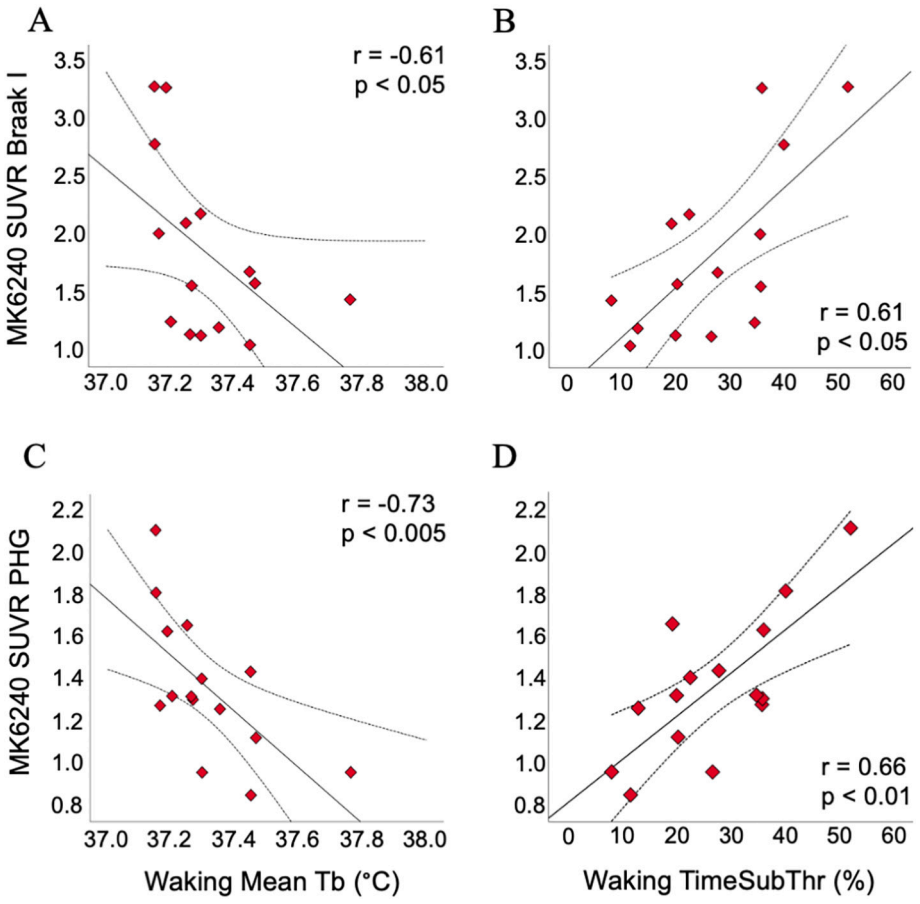

Fig. 5. | Associations between Waking Tb and MK-6240 SUVR uptake. A, C associations for mean Tb and MK6240 SUVR uptake in Braak I and parahippocampal gyrus regions, respectively. B, D, equivalent associations for the proportion of time Tb was under threshold during Waking intervals. Results of Spearman's rank correlations are shown, dashed lines show mean confidence intervals. Abbreviations, PHG, parahippocampal gyrus, Tb, body temperature, TimeSubThr, time Tb was under threshold, MK6240, [^{18}F]MK-6240 tau tangle tracer, SUVR, standardized uptake value ratio.

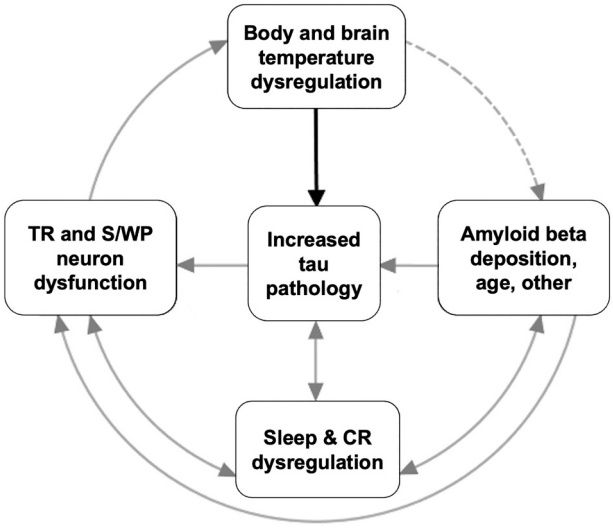

Fig. 6. | Bidirectional relationship between body and brain temperature dysregulation and tau pathology. Arm 1 (black arrow) represents a direct effect of body and brain temperature upon tau phosphorylation and other molecular targets affecting tau pathology. Arm 2 (grey arrows) represents a multifactorial pathway by which tau pathology impacts body and brain temperature. Dashed line indicates minimal data available. Abbreviations, TR, thermoregulatory, S/WP, sleep- or wake promoting (neuron), CR, circadian rhythm.

In general, little is known about how temperature variation within the physiological range influences neuronal function at the molecular level (Fig. 6, Arm 1). However, the relation between body temperature and brain tau phosphorylation is extensively documented in laboratory animals, including hibernating species. Temperature variation within the physiological range is strongly correlated with phosphorylation at Ser 202/Thr 205 used for Braak staging (Braak and Braak, 1997), and other sites including Thr 181 and Thr 231 that are hyperphosphorylated in AD (Planel et al., 2004; Planel et al., 2007; Bretteville et al., 2012; Arendt et al., 2003). In in vitro studies of human tau, temperature decrease from 37.4 °C to 36.3 °C robustly increases phosphorylation at these three sites (Guisle et al., 2020). Our study extends this body of evidence to in vivo measurements in humans. Molecular mechanisms other than phosphorylation may also contribute to the relation between temperature and tau pathology in AD. Circadian variation in Tb regulates alternative gene splicing via modulation of SR protein phosphorylation (Preussner et al., 2017), as well as neuronal expression of the tau chaperone hsp70 (Tsukamoto et al., 2019; Buhr et al., 2010), a process that prevents tau aggregation (Dickey et al., 2007; Kim et al., 2017). More generally, protein folding and ligand binding are known to be highly temperature-dependent (Fields et al., 2015; Hochachka and Somero, 1968; Somero et al., 2017; Somero, 1975; Somero and Low, 1976).

Associations between Tb and tau pathology may also arise from the effects of AD pathology upon thermoregulatory neurons (Fig. 6, Arm 2). Neuronal groups that exhibit NFTs in early AD include the dorsal raphe, suprachiasmatic nucleus, median preoptic area, and orexin-synthesizing neurons in the lateral hypothalamus (Braak et al., 2011; Rub et al., 2016;

Uematsu et al., 2018; Grinberg et al., 2009; Attems et al., 2012; Stratmann et al., 2016; Oh et al., 2019; Zhu et al., 2019; Swaab et al., 1992). All these groups have key thermoregulatory functions (Morrison and Nakamura, 2019; Tupone et al., 2011). The balance in causal flow between Arm 1 and Arm 2 may shift toward Arm 2 with AD progression, given that NFT burden in these neurons markedly increases with the onset of amyloid plaque deposition in medial temporal areas (Braak et al., 2011; Rub et al., 2016; Attems et al., 2012). Consistent with this scenario, various thermoregulatory disturbances have been reported in late-stage AD patients (Mishima et al., 1997; Harper et al., 2005; Prinz et al., 1984; Volicer et al., 2012; Harper et al., 2008; Satlin et al., 1995; Touitou et al., 1986; Okawa et al., 1991; Harper et al., 2004).

We found lower Waking Tb was associated with tau radiotracer uptake in Braak I–III regions, suggesting an association between lower Tb and pathological tau phosphorylation. By contrast, in laboratory animals, tau hyperphosphorylation in hippocampal and neocortical neurons observed during hypothermic states including hibernation (Arendt et al., 2003) and sleep (Guisle et al., 2020) was reversible. Nonetheless, persistent hypothermia (with tau phosphorylation) in older adults could contribute to tau aggregation, and AD-associated molecular defects may impair reversibility (Planel et al., 2009). Further longitudinal studies are required to test this. Our finding that lower Tb was associated with tau pathology during waking but not during sleep is consistent with the idea that temperature decrease during sleep is more likely to induce physiological (reversible) tau phosphorylation. While the function of hypothermia induced tau phosphorylation is not known, Arendt et al. proposed that tau phosphorylation may have a functional role in linking brain temperature decrease during entry into hibernation to neuroprotective remodeling of cytoskeletal and synaptic neuronal elements (Arendt et al., 2015; Arendt et al., 2003; Arendt and Bullmann, 2013). If tau phosphorylation during sleep or torpor was selected for in ancestral mammals, it may be that functionally related processes co-evolved to mitigate against aggregation. For example, Tb decrease upon sleep onset facilitates subsequent slow wave sleep (Shapiro et al., 1989; Horne and Staff, 1983; Jordan et al., 1990; Bunnell et al., 1988), which may increase tau clearance (Fultz et al., 2019; Rasmussen et al., 2018; Harrison et al., 2020; Holth et al., 2019).

A causal association between Tb dysregulation and tau pathology has therapeutic implications. Thermal interventions in older adults, for example hot baths or saunas, could prevent NFT formation. More frequent sauna bathing in middle-aged men is associated with halving of the risk of dementia in later years (Knekt et al., 2020), and in mice, sauna-like treatment robustly reduces tau phosphorylation via inducing mild hyperthermia (Guisle et al., 2022). Finally, targeting exercise toward raising Tb could help reverse some causes of hypothermia in older adults, including sedentary lifestyle and decreased muscle mass (Weitzman et al., 1982; Kenney and Munce, 2003; Blatteis, 2012; Gomolin et al., 2005; Weinert, 2010; Van Someren et al., 2002; Waalen and Buxbaum, 2011).

Our study has several limitations. The participant sample was relatively small, limiting statistical power, and was predominantly female Caucasian. Larger samples with more balanced demographics are required. Data on some potential confounds including habitual physical activity, amyloid status, and total tau levels were not collected and should be collected in future studies. While plasma and CSF P-tau were measured the day after Tb measurement, the interval between Tb measurement and tau PET scanning was variable. Although we did examine the effect of sleep vs waking state upon Tb–tau pathology associations, we did not determine whether these associations were confounded or mediated by sleep duration or other markers of sleep efficiency. Given evidence that the sleep-wake cycle affects tau levels in mice and human (Holth et al., 2019), this should be examined in future studies with larger sample size.

5. Conclusions

We report that lower Tb in cognitively normal older adults is associated with greater CSF and plasma P-tau levels, as well as greater tau MK6240 uptake in early Braak regions. This association was stronger in the waking state, suggesting an interaction between sleep wake state, body temperature and tau pathology. Our novel automated Tb data processing algorithm generated consistent temperature values, advancing the technique of Tb telemetry. Future studies are necessary to confirm these results, to examine whether additional related Tb features relate to tau pathology, and to assess the contribution of age, amyloid beta deposition, sleep impairment and *APOε4* status. Other important future directions include longitudinal studies to elucidate causality, and characterize the temporal dynamics between Tb variation and phosphorylation in soluble P-tau markers.

Ethics approval and consent to participate

Both the New York University Grossman School of Medicine and Icahn School of Medicine at Mount Sinai institutional review boards approved the inclusion of human participants for this study. All participants provided written informed consent.

Consent for publication

Both the New York University Grossman School of Medicine and Icahn School of Medicine at Mount Sinai institutional review boards approve the publication of anonymized study results from this cohort.

Availability of supporting data and code

Anonymized data and custom code written in Matlab version R2020b (Mathworks, Inc., Natick, MA) for DRAGO body temperature data preprocessing will be shared upon reasonable request.

Funding

This work was supported by grants from the NIH, including R21 AG055002, RF1AG057570, R56 AG058913, R01 AG012101, R01 AG022374, and R01 AG013616.

Credit author statement

Esther M. Blessing: NYU Grossman School of Medicine, designed and conceptualized study, analyzed the data, wrote the manuscript. Ankit Parekh: Icahn School of Medicine at Mount Sinai, designed and conceptualized study, acquired and analyzed the data, revised the manuscript. Rebecca A. Betensky: analyzed the data, revised the manuscript. James Babb: analyzed the data, revised the manuscript. Natalie Saba: analyzed the data, revised the manuscript. Ludovic Debure: Acquired and analyzed the data. Andrew W. Varga: Icahn School of Medicine at Mount Sinai, designed and conceptualized study, acquired and analyzed the data, revised the manuscript. Indu Ayappa: Icahn School of Medicine at Mount Sinai, designed and conceptualized study, revised the manuscript. David M. Rapoport: Icahn School of Medicine at Mount Sinai, designed and conceptualized study, revised the manuscript. Tracy A. Butler: Weill Cornell Medical College, acquired data, revised the manuscript. Mony J. de Leon: Weill Cornell Medical College, designed and conceptualized study, revised the manuscript. Thomas Wisniewski: NYU Grossman School of Medicine, designed and conceptualized study, revised the manuscript. Brian J. Lopresti: University of Pittsburgh, analyzed the data, revised the manuscript. Ricardo S. Osorio: NYU Grossman School of Medicine, designed and conceptualized study, acquired the data, analyzed the data, revised the manuscript. All authors read and approved the final manuscript.

Declaration of Competing Interest

The authors declare that they have no competing interests.

Acknowledgements

We thank Olivia Krivitsky and Zanetta Kovbasyuk for assistance with preparing figures and tables.

Appendix A. Supplementary data

Supplementary data to this article can be found online at https://doi.org/10.1016/j.nbd.2022.105748.

References

Arendt, T., Bullmann, T., 2013. Neuronal plasticity in hibernation and the proposed role of the microtubule-associated protein tau as a "master switch" regulating synaptic gain in neuronal networks. Am. J. Phys. Regul. Integr. Comp. Phys. 305, R478–R489.
Arendt, T., Holzer, M., Fruth, R., Bruckner, M.K., Gartner, U., 1995. Paired helical filament-like phosphorylation of tau, deposition of beta/A4-amyloid and memory impairment in rat induced by chronic inhibition of phosphatase 1 and 2A. Neuroscience 69, 691–698.
Arendt, T., et al., 2003. Reversible paired helical filament-like phosphorylation of tau is an adaptive process associated with neuronal plasticity in hibernating animals. J. Neurosci. 23, 6972–6981.
Arendt, T., Stieler, J., Holzer, M., 2015. Brain hypometabolism triggers PHF-like phosphorylation of tau, a major hallmark of Alzheimer's disease pathology. J. Neural Transm. (Vienna) 122, 531–539.
Aschoff, J., 1998. Circadian parameters as individual characteristics. J. Biol. Rhythm. 13, 123–131.
Attems, J., Thal, D.R., Jellinger, K.A., 2012. The relationship between subcortical tau pathology and Alzheimer's disease. Biochem. Soc. Trans. 40, 711–715.
Augustinack, J.C., Schneider, A., Mandelkow, E.M., Hyman, B.T., 2002. Specific tau phosphorylation sites correlate with severity of neuronal cytopathology in Alzheimer's disease. Acta Neuropathol. 103, 26–35.
Barthelemy, N.R., et al., 2020. A soluble phosphorylated tau signature links tau, amyloid and the evolution of stages of dominantly inherited Alzheimer's disease. Nat. Med. 26, 398–407.
Betthauser, T.J., et al., 2020. Amyloid and tau imaging biomarkers explain cognitive decline from late middle-age. Brain 143, 320–335.
Biundo, F., Del Prete, D., Zhang, H., Arancio, O., D'Adamio, L., 2018. A role for tau in learning, memory and synaptic plasticity. Sci. Rep. 8, 3184.
Blatteis, C.M., 2012. Age-dependent changes in temperature regulation - a mini review. Gerontology 58, 289–295.
Braak, H., Braak, E., 1997. Frequency of stages of Alzheimer-related lesions in different age categories. Neurobiol. Aging 18, 351–357.
Braak, H., Thal, D.R., Ghebremedhin, E., Del Tredici, K., 2011. Stages of the pathologic process in Alzheimer disease: age categories from 1 to 100 years. J. Neuropathol. Exp. Neurol. 70, 960–969.
Bretteville, A., et al., 2012. Hypothermia-induced hyperphosphorylation: a new model to study tau kinase inhibitors. Sci. Rep. 2, 480.
Buhr, E.D., Yoo, S.H., Takahashi, J.S., 2010. Temperature as a universal resetting cue for mammalian circadian oscillators. Science 330, 379–385.
Bunnell, D.E., Agnew, J.A., Horvath, S.M., Jopson, L., Wills, M., 1988. Passive body heating and sleep: influence of proximity to sleep. Sleep 11, 210–219.
Byrne, C., Lim, C.L., 2007. The ingestible telemetric body core temperature sensor: a review of validity and exercise applications. Br. J. Sports Med. 41, 126–133.
Casa, D.J., et al., 2007. Validity of devices that assess body temperature during outdoor exercise in the heat. J. Athl. Train. 42, 333–342.
Clark, C., et al., 2021. Plasma neurofilament light and phosphorylated tau 181 as biomarkers of Alzheimer's disease pathology and clinical disease progression. Alzheimers Res. Ther. 13, 65.
Czeisler, C.A., Zimmerman, J.C., Ronda, J.M., Moore-Ede, M.C., Weitzman, E.D., 1980. Timing of REM sleep is coupled to the circadian rhythm of body temperature in man. Sleep 2, 329–346.
Dickey, C.A., et al., 2007. The high-affinity HSP90-CHIP complex recognizes and selectively degrades phosphorylated tau client proteins. J. Clin. Invest. 117, 648–658.
Dixit, R., Ross, J.L., Goldman, Y.E., Holzbaur, E.L., 2008. Differential regulation of dynein and kinesin motor proteins by tau. Science 319, 1086–1089.
Duffy, J.F., Dijk, D.J., 2002. Getting through to circadian oscillators: why use constant routines? J. Biol. Rhythm. 17, 4–13.
Fields, P.A., Dong, Y., Meng, X., Somero, G.N., 2015. Adaptations of protein structure and function to temperature: there is more than one way to 'skin a cat'. J. Exp. Biol. 218, 1801–1811.
Fultz, N.E., et al., 2019. Coupled electrophysiological, hemodynamic, and cerebrospinal fluid oscillations in human sleep. Science 366, 628–631.
Gant, N., Atkinson, G., Williams, C., 2006. The validity and reliability of intestinal temperature during intermittent running. Med. Sci. Sports Exerc. 38, 1926–1931.
Gogola, A., et al., 2021. Direct comparison of the tau PET tracers [(18)F]flortaucipir and [(18)F]MK-6240 in human subjects. J. Nucl. Med. 63, 108–116.
Gomolin, I.H., Aung, M.M., Wolf-Klein, G., Auerbach, C., 2005. Older is colder: temperature range and variation in older people. J. Am. Geriatr. Soc. 53, 2170–2172.
Gong, C.X., Iqbal, K., 2008. Hyperphosphorylation of microtubule-associated protein tau: a promising therapeutic target for Alzheimer disease. Curr. Med. Chem. 15, 2321–2328.
Gong, C.X., Liu, F., Grundke-Iqbal, I., Iqbal, K., 2005. Post-translational modifications of tau protein in Alzheimer's disease. J. Neural Transm. (Vienna) 112, 813–838.
Gotz, J., Halliday, G., Nisbet, R.M., 2019. Molecular pathogenesis of the Tauopathies. Annu. Rev. Pathol. 14, 239–261.
Gratuze, M., Julien, J., Petry, F.R., Morin, F., Planel, E., 2017. Insulin deprivation induces PP2A inhibition and tau hyperphosphorylation in hTau mice, a model of Alzheimer's disease-like tau pathology. Sci. Rep. 7, 46359.
Grinberg, L.T., et al., 2009. The dorsal raphe nucleus shows phospho-tau neurofibrillary changes before the transentorhinal region in Alzheimer's disease. A precocious onset? Neuropathol. Appl. Neurobiol. 35, 406–416.
Grundke-Iqbal, I., et al., 1986. Abnormal phosphorylation of the microtubule-associated protein tau (tau) in Alzheimer cytoskeletal pathology. Proc. Natl. Acad. Sci. U. S. A. 83, 4913–4917.
Guisle, I., et al., 2020. Circadian and sleep/wake-dependent variations in tau phosphorylation are driven by temperature. Sleep 43, 1–12.
Guisle, I., et al., 2022. Sauna-like conditions or menthol treatment reduce tau phosphorylation through mild hyperthermia. Neurobiol. Aging 113, 118–130.
Guo, T., Noble, W., Hanger, D.P., 2017. Roles of tau protein in health and disease. Acta Neuropathol. 133, 665–704.
Hansson, O., et al., 2006. Association between CSF biomarkers and incipient Alzheimer's disease in patients with mild cognitive impairment: a follow-up study. Lancet Neurol. 5, 228–234.
Hansson, O., et al., 2018. CSF biomarkers of Alzheimer's disease concord with amyloid-beta PET and predict clinical progression: a study of fully automated immunoassays in BioFINDER and ADNI cohorts. Alzheimers Dement. 14, 1470–1481.
Harper, D.G., et al., 2004. Dementia severity and Lewy bodies affect circadian rhythms in Alzheimer disease. Neurobiol. Aging 25, 771–781.
Harper, D.G., et al., 2005. Disturbance of endogenous circadian rhythm in aging and Alzheimer disease. Am. J. Geriatr. Psychiatry 13, 359–368.
Harper, D.G., et al., 2008. Dorsomedial SCN neuronal subpopulations subserve different functions in human dementia. Brain 131, 1609–1617.
Harrison, I.F., et al., 2020. Impaired glymphatic function and clearance of tau in an Alzheimer's disease model. Brain 143, 2576–2593.
Hitrec, T., et al., 2021. Reversible tau phosphorylation induced by synthetic torpor in the spinal cord of the rat. Front. Neuroanat. 15, 592288.
Hochachka, P.W., Somero, G.N., 1968. The adaptation of enzymes to temperature. Comp. Biochem. Physiol. 27, 659–668.
Holth, J.K., et al., 2019. The sleep-wake cycle regulates brain interstitial fluid tau in mice and CSF tau in humans. Science 363, 880–884.
Horne, J.A., Staff, L.H., 1983. Exercise and sleep: body-heating effects. Sleep 6, 36–46.
Hostetler, E.D., et al., 2016. Preclinical characterization of 18F-MK-6240, a promising PET tracer for in vivo quantification of human neurofibrillary tangles. J. Nucl. Med. 57, 1599–1606.
Huang, Q., Komarzynski, S., Bolborea, M., Finkenstadt, B., Levi, F.A., 2021. Telemonitored human circadian temperature dynamics during daily routine. Front. Physiol. 12, 659973.
Janelidze, S., et al., 2020. Plasma P-tau181 in Alzheimer's disease: relationship to other biomarkers, differential diagnosis, neuropathology and longitudinal progression to Alzheimer's dementia. Nat. Med. 26, 379–386.
Johns, M.W., 1991. A new method for measuring daytime sleepiness: the Epworth sleepiness scale. Sleep 14, 540–545.
Jordan, J., Montgomery, I., Trinder, J., 1990. The effect of afternoon body heating on body temperature and slow wave sleep. Psychophysiology 27, 560–566.
Karikari, T.K., et al., 2020. Blood phosphorylated tau 181 as a biomarker for Alzheimer's disease: a diagnostic performance and prediction modelling study using data from four prospective cohorts. Lancet Neurol. 19, 422–433.
Kelly, G., 2006. Body temperature variability (part 1): a review of the history of body temperature and its variability due to site selection, biological rhythms, fitness, and aging. Altern. Med. Rev. 11, 278–293.
Kelly, G.S., 2007. Body temperature variability (part 2): masking influences of body temperature variability and a review of body temperature variability in disease. Altern. Med. Rev. 12, 49–62.
Kenney, W.L., Munce, T.A., 2003. Invited review: aging and human temperature regulation. J. Appl. Physiol. 1985 (95), 2598–2603.
Kim, E., Sakata, K., Liao, F.F., 2017. Bidirectional interplay of HSF1 degradation and UPR activation promotes tau hyperphosphorylation. PLoS Genet. 13, e1006849.
Kimura, T., et al., 2014. Microtubule-associated protein tau is essential for long-term depression in the hippocampus. Philos. Trans. R. Soc. Lond. Ser. B Biol. Sci. 369, 20130144.
Knekt, P., Jarvinen, R., Rissanen, H., Heliovaara, M., Aromaa, A., 2020. Does sauna bathing protect against dementia? Prev. Med. Rep. 20, 101221.
Krauchi, K., Wirz-Justice, A., 1994. Circadian rhythm of heat production, heart rate, and skin and core temperature under unmasking conditions in men. Am. J. Phys. 267, R819–R829.
Laing, K.K., et al., 2020. Cerebrovascular disease promotes tau pathology in Alzheimer's disease. Brain Commun. 2, fcaa132.
Lee, J., et al., 2020. Cerebrospinal fluid biomarkers for the diagnosis and classification of Alzheimer's disease Spectrum. J. Korean Med. Sci. 35, e361.

Lindwall, G., Cole, R.D., 1984. Phosphorylation affects the ability of tau protein to promote microtubule assembly. J. Biol. Chem. 259, 5301–5305.
Luppi, M., et al., 2019. Phosphorylation and Dephosphorylation of tau protein during synthetic torpor. Front. Neuroanat. 13, 57.
Mishima, K., et al., 1997. Different manifestations of circadian rhythms in senile dementia of Alzheimer's type and multi-infarct dementia. Neurobiol. Aging 18, 105–109.
Monnard, C.R., et al., 2017. Issues in continuous 24-h Core body temperature monitoring in humans using an ingestible capsule telemetric sensor. Front Endocrinol (Lausanne) 8, 130.
Morrison, S.F., Nakamura, K., 2019. Central mechanisms for thermoregulation. Annu. Rev. Physiol. 81, null.
Oh, J., et al., 2019. Profound degeneration of wake-promoting neurons in Alzheimer's disease. Alzheimers Dement. 15, 1253–1263.
Okawa, M., et al., 1991. Circadian rhythm disorders in sleep-waking and body temperature in elderly patients with dementia and their treatment. Sleep 14, 478–485.
Ossenkoppele, R., et al., 2016. Tau PET patterns mirror clinical and neuroanatomical variability in Alzheimer's disease. Brain 139, 1551–1567.
Ossenkoppele, R., et al., 2021. Accuracy of tau positron emission tomography as a prognostic marker in preclinical and prodromal Alzheimer disease: a head-to-head comparison against amyloid positron emission tomography and magnetic resonance imaging. JAMA Neurol. 78, 961–971.
Parekh, A., 2021. In: Obeid, I., Selesnick, I., Picone, J. (Eds.), Nonlinear Smoothing of Core Body Temperature Data with Random Gaps and Outliers (DRAGO). In *Biomedical Signal Processing*. Springer International Publishing, pp. 63–84.
Pascoal, T.A., et al., 2017. Amyloid-beta and hyperphosphorylated tau synergy drives metabolic decline in preclinical Alzheimer's disease. Mol. Psychiatry 22, 306–311.
Pascoal, T.A., et al., 2018. In vivo quantification of neurofibrillary tangles with [(18)F] MK-6240. Alzheimers Res. Ther. 10, 74.
Pascoal, T.A., et al., 2020. 18F-MK-6240 PET for early and late detection of neurofibrillary tangles. Brain 143, 2818–2830.
Planel, E., Yasutake, K., Fujita, S.C., Ishiguro, K., 2001. Inhibition of protein phosphatase 2A overrides tau protein kinase I/glycogen synthase kinase 3 beta and cyclin-dependent kinase 5 inhibition and results in tau hyperphosphorylation in the hippocampus of starved mouse. J. Biol. Chem. 276, 34298–34306.
Planel, E., et al., 2004. Alterations in glucose metabolism induce hypothermia leading to tau hyperphosphorylation through differential inhibition of kinase and phosphatase activities: implications for Alzheimer's disease. J. Neurosci. 24, 2401–2411.
Planel, E., et al., 2007. Anesthesia leads to tau hyperphosphorylation through inhibition of phosphatase activity by hypothermia. J. Neurosci. 27, 3090–3097.
Planel, E., et al., 2008. Anesthesia-induced hyperphosphorylation detaches 3-repeat tau from microtubules without affecting their stability in vivo. J. Neurosci. 28, 12798–12807.
Planel, E., et al., 2009. Acceleration and persistence of neurofibrillary pathology in a mouse model of tauopathy following anesthesia. FASEB J. 23, 2595–2604.
Preussner, M., et al., 2017. Body temperature cycles control rhythmic alternative splicing in mammals. Mol. Cell 67, 433–446 e434.
Prinz, P.N., et al., 1984. Circadian temperature variation in healthy aged and in Alzheimer's disease. J. Gerontol. 39, 30–35.
Rasmussen, M.K., Mestre, H., Nedergaard, M., 2018. The glymphatic pathway in neurological disorders. Lancet Neurol. 17, 1016–1024.
Refinetti, R., 2010. The circadian rhythm of body temperature. Front Biosci. (Landmark Ed) 15, 564–594.
Refinetti, R., Lissen, G.C., Halberg, F., 2007. Procedures for numerical analysis of circadian rhythms. Biol. Rhythm. Res. 38, 275–325.
Rousset, O.G., Ma, Y., Evans, A.C., 1998. Correction for partial volume effects in PET: principle and validation. J. Nucl. Med. 39, 904–911.
Rub, U., et al., 2016. The brainstem tau cytoskeletal pathology of Alzheimer's disease: a brief historical overview and description of its anatomical distribution pattern, evolutional features, Pathogenetic and clinical relevance. Curr. Alzheimer Res. 13, 1178–1197.
Satlin, A., Volicer, L., Stopa, E.G., Harper, D., 1995. Circadian locomotor activity and core-body temperature rhythms in Alzheimer's disease. Neurobiol. Aging 16, 765–771.
Scheltens, P., et al., 2021. Alzheimer's disease. Lancet 397, 1577–1590.
Shapiro, C.M., Allan, M., Driver, H., Mitchell, D., 1989. Thermal load alters sleep. Biol. Psychiatry 26, 736–740.
Shukla, V., Skuntz, S., Pant, H.C., 2012. Deregulated Cdk5 activity is involved in inducing Alzheimer's disease. Arch. Med. Res. 43, 655–662.
Somero, G.N., 1975. Temperature as a selective factor in protein evolution: the adaptational strategy of "compromise". J. Exp. Zool. 194, 175–188.
Somero, G.N., Low, P.S., 1976. Temperature: a 'shaping force' in protein evolution. Biochem. Soc. Symp. 33–42.
Somero, G.N., Lockwood, B.L., Tomanek, L., 2017. Biochemical Adaptation : Response to Environmental Challenges, from life's Origins to the Anthropocene. Sinauer Associates, Inc. Publishers, Sunderland, Massachusetts.
Sontag, J.M., Sontag, E., 2014. Protein phosphatase 2A dysfunction in Alzheimer's disease. Front. Mol. Neurosci. 7, 16.
Spiegel, J., et al., 2016. Greater specificity for cerebrospinal fluid P-tau231 over P-tau181 in the differentiation of healthy controls from Alzheimer's disease. J. Alzheimer's Dis. : JAD 49, 93–100.
Stieler, J.T., et al., 2011. The physiological link between metabolic rate depression and tau phosphorylation in mammalian hibernation. PLoS One 6, e14530.
Stratmann, K., et al., 2016. Precortical phase of Alzheimer's disease (AD)-related tau cytoskeletal pathology. Brain Pathol. 26, 371–386.
Sund-Levander, M., Forsberg, C., Wahren, L.K., 2002. Normal oral, rectal, tympanic and axillary body temperature in adult men and women: a systematic literature review. Scand. J. Caring Sci. 16, 122–128.
Swaab, D.F., et al., 1992. Tau and ubiquitin in the human hypothalamus in aging and Alzheimer's disease. Brain Res. 590, 239–249.
Touitou, Y., et al., 1986. Age-related changes in both circadian and seasonal rhythms of rectal temperature with special reference to senile dementia of Alzheimer type. Gerontology 32, 110–118.
Tournissac, M., Vandal, M., Francois, A., Planel, E., Calon, F., 2017. Old age potentiates cold-induced tau phosphorylation: linking thermoregulatory deficit with Alzheimer's disease. Neurobiol. Aging 50, 25–29.
Tournissac, M., et al., 2019. Repeated cold exposures protect a mouse model of Alzheimer's disease against cold-induced tau phosphorylation. Mol. Metab. 22, 110–120.
Travers, G.J., Nichols, D.S., Farooq, A., Racinais, S., Periard, J.D., 2016. Validation of an ingestible temperature data logging and telemetry system during exercise in the heat. Temperature (Austin) 3, 208–219.
Tsukamoto, D., et al., 2019. Circadian transcription factor HSF1 regulates differential HSP70 gene transcription during the arousal-torpor cycle in mammalian hibernation. Sci. Rep. 9, 832.
Tupone, D., Madden, C.J., Cano, G., Morrison, S.F., 2011. An orexinergic projection from perifornical hypothalamus to raphe pallidus increases rat brown adipose tissue thermogenesis. J. Neurosci. 31, 15944–15955.
Uematsu, M., et al., 2018. Brainstem tau pathology in Alzheimer's disease is characterized by increase of three repeat tau and independent of amyloid beta. Acta Neuropathol. Commun. 6, 1.
van der Kant, R., Goldstein, L.S.B., Ossenkoppele, R., 2020. Amyloid-beta-independent regulators of tau pathology in Alzheimer disease. Nat. Rev. Neurosci. 21, 21–35.
Van Someren, E.J., Raymann, R.J., Scherder, E.J., Daanen, H.A., Swaab, D.F., 2002. Circadian and age-related modulation of thermoreception and temperature regulation: mechanisms and functional implications. Ageing Res. Rev. 1, 721–778.
Vandal, M., et al., 2016. Impaired thermoregulation and beneficial effects of thermoneutrality in the 3xTg-AD model of Alzheimer's disease. Neurobiol. Aging 43, 47–57.
Vanderstichele, H., et al., 2012. Standardization of preanalytical aspects of cerebrospinal fluid biomarker testing for Alzheimer's disease diagnosis: a consensus paper from the Alzheimer's biomarkers standardization initiative. Alzheimers Dement. 8, 65–73.
Vershinin, M., Carter, B.C., Razafsky, D.S., King, S.J., Gross, S.P., 2007. Multiple-motor based transport and its regulation by tau. Proc. Natl. Acad. Sci. U. S. A. 104, 87–92.
Volicer, L., Harper, D.G., Stopa, E.G., 2012. Severe impairment of circadian rhythm in Alzheimer's disease. J. Nutr. Health Aging 16, 888–890.
Waalen, J., Buxbaum, J.N., 2011. Is older colder or colder older? The association of age with body temperature in 18,630 individuals. J. Gerontol. A Biol. Sci. Med. Sci. 66, 487–492.
Wegmann, S., Biernat, J., Mandelkow, E., 2021. A current view on tau protein phosphorylation in Alzheimer's disease. Curr. Opin. Neurobiol. 69, 131–138.
Weinert, D., 2010. Circadian temperature variation and ageing. Ageing Res. Rev. 9, 51–60.
Weitzman, E.D., Moline, M.L., Czeisler, C.A., Zimmerman, J.C., 1982. Chronobiology of aging: temperature, sleep-wake rhythms and entrainment. Neurobiol. Aging 3, 299–309.
Yap, S.Y., et al., 2021. Discriminatory ability of next-generation tau PET tracers for Alzheimer's disease. Brain 144, 2284–2290.
Zhu, K., et al., 2019. Primary age-related Tauopathy in human subcortical nuclei. Front. Neurosci. 13, 529.